

PHYSICAL REVIEW C

NUCLEAR PHYSICS

THIRD SERIES, VOLUME 27, NUMBER 6

JUNE 1983

$n + {}^6\text{Li}$ system investigated with the resonating-group method: Effects of target clustering and charge form factor

Y. Fujiwara and Y. C. Tang

School of Physics, University of Minnesota, Minneapolis, Minnesota 55455

(Received 21 January 1983)

The influence of the clustering and charge-form-factor behavior of ${}^6\text{Li}$ on the properties of the $n + {}^6\text{Li}$ system is investigated. By examining the $n + {}^6\text{Li}$ cross-section and phase-shift results, it is found that, in the low-energy region, a proper consideration of $d + \alpha$ cluster correlations in ${}^6\text{Li}$ is essential to explain the resonance structure, while in the high-energy region one must adopt in the calculation a ${}^6\text{Li}$ internal function which yields the empirical form-factor values over a wide q^2 range. Contributions from various nucleon-exchange terms are also studied. Here one finds that the main characteristics of these contributions do not seem to depend sensitively on the detailed nature of the cluster internal function.

NUCLEAR REACTIONS ${}^6\text{Li}(n,n)$. Effects of target clustering and charge form factor. Resonating-group method with three-cluster formulation.

I. INTRODUCTION

Within the past two or three decades, the resonating-group method (RGM) (Refs. 1–5) has been extensively used to microscopically study the behavior of many nuclear systems. Because of computational complexities, however, refined calculations have generally been performed only for light two-cluster systems⁶ consisting of s -shell N , d , ${}^3\text{H}$, ${}^3\text{He}$, and α clusters. When heavier clusters are involved, it was frequently found necessary to adopt the assumption of choosing very simple wave functions for the description of their internal structures. With such a simplifying assumption, one cannot, of course, expect to achieve a proper account of the charge-form-factor behavior or the nucleon-density distribution. In addition, cluster correlations which are particularly prominent in the nuclear surface region cannot be taken into consideration. For instance, in the investigation of the ${}^{16}\text{O} + {}^{28}\text{Si}$ system by Langanke,⁷ the ${}^{16}\text{O}$ and ${}^{28}\text{Si}$ nuclei were assumed to occupy the lowest configurations in harmonic-

oscillator wells of equal width parameter. Undoubtedly, the use of these simple configurations reduced the computational effort to a large extent, but the calculation does suffer the consequence that the results obtained can be viewed to have only qualitative significance.

In this investigation, we wish to examine the question concerning the importance of choosing, in RGM calculations, internal functions which properly describe the charge-form-factor behavior and take into account cluster correlations within the projectile and the target nuclei. For this purpose, we shall consider in a systematic manner the $n + {}^6\text{Li}$ system as a test example. We choose this particular system for a detailed study, not only because it is a comparatively simple system from a computational viewpoint, but also because charge-form-factor values for ${}^6\text{Li}$ have been measured over a wide q^2 range⁸ and because this target nucleus is known to have a large degree of $d + \alpha$ clustering.⁹ What we propose to do is to compute the $n + {}^6\text{Li}$ phase shifts and scattering angular distributions with a number

of suitably chosen ${}^6\text{Li}$ internal functions which differ from one another in regard to the form-factor behavior and the degree of $d + \alpha$ cluster correlation. In other words, we plan to explore the possibility of adopting the neutron as a probe to study the internal structure of ${}^6\text{Li}$. By comparing the results calculated for the above-mentioned quantities, we can then obtain some quantitative measure of the effects associated with the nucleon density distribution and the cluster structure of the target nucleus.

To continue our series of studies aimed at a detailed understanding of the importance of intercluster antisymmetrization,^{10,11} we also examine exchange effects in this investigation. The main purpose is, of course, to see in what way cluster correlations in the target nucleus affect the contributions from the various nucleon-exchange terms.

In Sec. II, we describe the types of ${}^6\text{Li}$ internal wave functions to be used in this study and give a brief description of the $n + {}^6\text{Li}$ single-channel resonating-group formulation. Results are presented in Sec. III, where the emphasis will be on discussing the influence of the ${}^6\text{Li}$ charge form factor and $d + \alpha$ cluster correlations on the properties of the $n + {}^6\text{Li}$ system. In Sec. IV, we examine the effects of various nucleon-exchange terms; we shall show that the conclusions regarding class A and class B terms, summarized in Ref. 11, remain valid even when the target nucleus contains an appreciable degree of nucleon clustering. Finally, in Sec. V, we summarize the essential findings of this investigation and make some concluding remarks.

II. FORMULATION

A. Internal wave function of ${}^6\text{Li}$

The following two types of ${}^6\text{Li}$ internal wave functions will be used in this investigation:

(i) *A type I function which describes ${}^6\text{Li}$ as having an appreciable degree of surface clustering.*¹² Three wave functions of this type will be considered; these are

$$\phi_i = N_i \mathcal{A}[\tilde{\phi}_i \tilde{\xi} \tilde{Z}(\vec{R}_6)], \quad (i = 1, 2, 3), \quad (1)$$

where \mathcal{A} is an antisymmetrization operator, $\tilde{\xi}$ is a spin-isospin function appropriate for the ground state, N_i is a normalization factor, and \tilde{Z} is a function describing the c.m. motion of ${}^6\text{Li}$. To account for the presence of $d + \alpha$ clustering, we use

$$\tilde{\phi}_i = \phi_\alpha \phi_d \chi_i(\vec{r}), \quad (2)$$

where ϕ_α and ϕ_d describe the internal spatial structures of the α and d clusters, given by

$$\phi_\alpha = \left[\frac{\alpha^3}{4\pi^3} \right]^{3/4} \exp \left[-\frac{1}{2} \alpha \sum_{i=1}^4 (\vec{r}_i - \vec{R}_\alpha)^2 \right], \quad (3)$$

$$\phi_d = \left[\frac{\bar{\alpha}}{2\pi} \right]^{3/4} \exp \left[-\frac{1}{2} \bar{\alpha} \sum_{i=5}^6 (\vec{r}_i - \vec{R}_d)^2 \right], \quad (4)$$

with \vec{R}_α and \vec{R}_d being, respectively, the c.m. coordinates of the α and d clusters. The width parameter α is chosen as 0.514 fm^{-2} to correctly yield the empirically determined rms radius of 1.48 fm for the α particle.¹³ As for the choice of $\bar{\alpha}$, we take into consideration a recent finding¹⁴ that the deuteron cluster in ${}^6\text{Li}$ is appreciably compressed. Thus, as a reasonable approximation, we choose $\bar{\alpha}$ to be equal to α . It should be mentioned that, with this simplifying choice, the effort required to derive the analytical expression of the three cluster $n + d + \alpha$ kernel in the $n + {}^6\text{Li}$ problem is also substantially reduced.

The relative-motion function $\chi_i(\vec{r})$ in Eq. (2) is chosen to have the form

$$\chi_1(\vec{r}) = \exp(-\frac{2}{3} \beta_1 \alpha r^2) + c_1 \exp(-\frac{2}{3} \gamma_1 \alpha r^2), \quad (5)$$

with three adjustable parameters β_1 , γ_1 , and c_1 , or

$$\chi_2(\vec{r}) = (1 + c_2 \alpha r^2) \exp(-\frac{2}{3} \beta_2 \alpha r^2), \quad (6)$$

with two adjustable parameters β_2 and c_2 , or

$$\chi_3(\vec{r}) = r^2 \exp(-\frac{2}{3} \beta_3 \alpha r^2), \quad (7)$$

with only a single adjustable parameter β_3 . These parameters are then adjusted according to the charge-form-factor data up to q^2 values of about 6 fm^{-2} , subject to the condition that the empirically determined rms charge radius of 2.51 fm (Ref. 8) be reproduced. The results are

$$\beta_1 = 0.0841, \quad \gamma_1 = 0.60, \quad c_1 = 2.337, \quad (8)$$

$$\beta_2 = 0.1464, \quad c_2 = -0.1234, \quad (9)$$

$$\beta_3 = 0.387, \quad (10)$$

and the fits to the empirical F_{ch}^2 data are shown in Fig. 1. Here it is seen that both ϕ_1 and ϕ_2 yield satisfactory results. On the other hand, because the single parameter β_3 in ϕ_3 is already constrained to yield the correct rms radius, the fit with ϕ_3 becomes necessarily rather poor in the higher- q^2 region.

(ii) *A type II function which describes a shell-model-like structure for ${}^6\text{Li}$ with little surface clustering.* Two wave functions of this type (ϕ_4 and ϕ_5) will be examined. These are given by Eq. (1), but with

$$\tilde{\phi}_4 = (\vec{r}_5 - \vec{R}_6) \cdot (\vec{r}_6 - \vec{R}_6) \left\{ \exp \left[-\frac{1}{2} \beta_4 \sum_{i=1}^6 (\vec{r}_i - \vec{R}_6)^2 \right] + c_4 \exp \left[-\frac{1}{2} \gamma_4 \sum_{i=1}^6 (\vec{r}_i - \vec{R}_6)^2 \right] \right\}, \quad (11)$$

$$\tilde{\phi}_5 = (\vec{r}_5 - \vec{R}_6) \cdot (\vec{r}_6 - \vec{R}_6) \exp \left[-\frac{1}{2} \beta_5 \sum_{i=1}^6 (\vec{r}_i - \vec{R}_6)^2 \right], \quad (12)$$

where the parameters are

$$\begin{aligned} \beta_4 &= 0.169 \text{ fm}^{-2}, \\ \gamma_4 &= 0.458 \text{ fm}^{-2}, \end{aligned} \quad (13)$$

$$\begin{aligned} c_4 &= 145.1, \\ \beta_5 &= 0.278 \text{ fm}^{-2}. \end{aligned} \quad (14)$$

The internal function ϕ_4 has already been studied in a previous publication,¹⁵ and the calculated charge-form-factor behavior is depicted by the solid curve in Fig. 1 there. The function ϕ_5 represents a translationally-invariant shell-model function having the most space-symmetric $(1s)^4(1p)^2$ configuration in a harmonic-oscillator well. The choice of 0.278 fm^{-2} for the width parameter β_5 is dictated by our desire to obtain the correct ${}^6\text{Li}$ rms charge radius. With this choice, the result for the calculated form factor is shown also in Fig. 1; as expected, the fit to experiment in the higher- q^2 region is not of good quality due to the lack of flexibility in this wave function.

Characteristic differences between type I and type II functions show up in the following ways:

(i) The overlap Q_{ij} , defined as

$$Q_{ij} = |\langle \phi_i | \phi_j \rangle|^2, \quad (15)$$

is calculated to be

$$\begin{aligned} Q_{15} &= 0.568, \quad Q_{25} = 0.566, \\ Q_{35} &= 0.546, \quad Q_{45} = 0.837. \end{aligned} \quad (16)$$

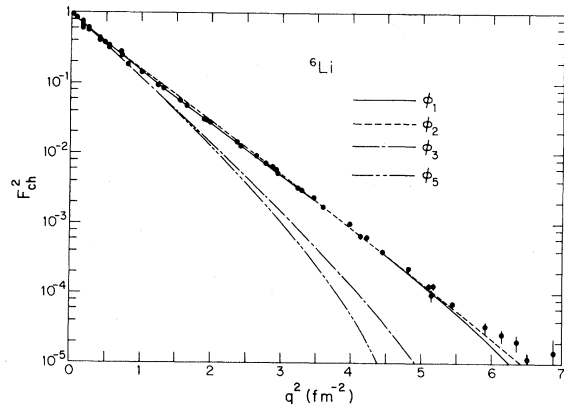


FIG. 1. Charge form factors of ${}^6\text{Li}$ calculated with various internal functions.

Here it is seen that the overlap between the two type II functions ϕ_4 and ϕ_5 is comparatively large, indicating the similarity in their gross structures. On the other hand, the overlap between the type I (ϕ_1 , ϕ_2 , or ϕ_3) and type II (ϕ_5) functions is considerably smaller, having a value of only around 0.55.

(ii) The reduced width amplitude $\tilde{\mathcal{Y}}_0^i$, defined as

$$\tilde{\mathcal{Y}}_0^i(r) = \left[\begin{matrix} 6 \\ 2 \end{matrix} \right]^{1/2} r \langle \phi_\alpha \phi_d \tilde{\xi} \tilde{Z} Y_0^0(\hat{r}) | \phi_i \rangle, \quad (17)$$

is shown in Fig. 2.¹⁶ From this figure, one notes that for the type I function ϕ_1 , ϕ_2 , or ϕ_3 , this amplitude has a large magnitude in the region where the separation distance r is around 6 fm. This is in contrast to the situation with ϕ_5 where the amplitude $\tilde{\mathcal{Y}}_0^5$ becomes quite small for large r values.

The above discussion shows that type I and type II functions are structurally dissimilar, mainly due to the different degree of $d + \alpha$ clustering.¹⁷ It is the purpose of this investigation to find out how such a structure difference can be revealed by using the neutron as a probe.

For convenience of discussion, we shall further designate ϕ_1 , ϕ_2 , and ϕ_4 as type A functions which yield correct form-factor values for q^2 up to 6 fm^{-2} , and ϕ_3 and ϕ_5 as type B functions which give the correct rms radius but a poor representation of the form-factor behavior in the higher- q^2 region.

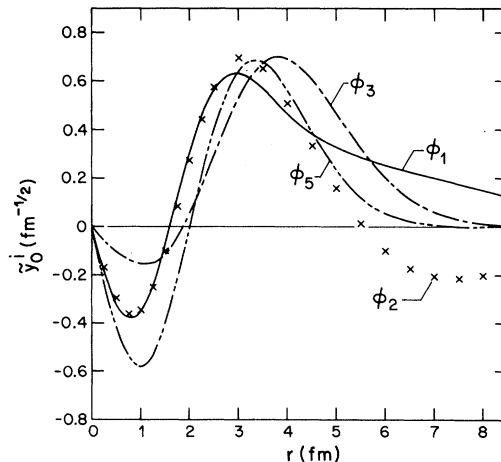


FIG. 2. Reduced width amplitudes for $d + \alpha$ clustering in ${}^6\text{Li}$.

B. Formulation of the $n + {}^6\text{Li}$ problem

The formulation of a single-channel resonating-group calculation has been discussed in detail elsewhere^{1,3}; hence, only a very brief description will be given here. The trial wave function for the $n + {}^6\text{Li}$ system is written as

$$\psi_{i\lambda} = \mathcal{A}[\tilde{\phi}_i F_{i\lambda}(\vec{R}) \xi_\lambda Z(\vec{R}_{c.m.})], \quad (18)$$

where ξ_λ is an appropriate spin-isospin function and $Z(\vec{R}_{c.m.})$ is a function describing the total c.m. motion. The subscript λ denotes the channel-spin multiplicity $(2s + 1)$, with s being the channel spin angular-momentum quantum number of the system which can be either $\frac{3}{2}$ or $\frac{1}{2}$. The function $F_{i\lambda}(\vec{R})$ represents the relative motion of the neutron and the ${}^6\text{Li}$ cluster. It satisfies an integrodifferential equation, the solution of which yields the phase shift ${}^\lambda\delta_l$ and the scattering differential cross section $\sigma(\theta)$.

The nucleon-nucleon potential used is given by Eqs. (9)–(11) of a previous publication.¹⁸ The exchange-mixture parameter u is taken to be 1. For simplicity in calculation, we have also omitted the small exchange-Coulomb contribution by letting the charge of the proton be infinitesimally small.

The central quantities in a resonating-group calculation are the normalization and Hamiltonian kernels [see Eqs. (14), (15), (42), and (43) of Ref. 3]. In this study, we first analytically derive the three-cluster normalization kernel $\tilde{\mathcal{N}}_{i\lambda}(\vec{r}', \vec{R}'; \vec{r}'', \vec{R}'')$ and the three-cluster Hamiltonian kernel $\tilde{\mathcal{H}}_{i\lambda}(\vec{r}', \vec{R}'; \vec{r}'', \vec{R}'')$. By folding in the $d + \alpha$ relative-motion function, we then obtain the $n + {}^6\text{Li}$ two-cluster kernels $\mathcal{N}_{i\lambda}(\vec{R}', \vec{R}'')$ and $\mathcal{H}_{i\lambda}(\vec{R}', \vec{R}'')$.¹⁹ These latter kernels consist of many terms, but may be classified into 1a, 1c, and 1d groups. This particular grouping is convenient, because in the limit

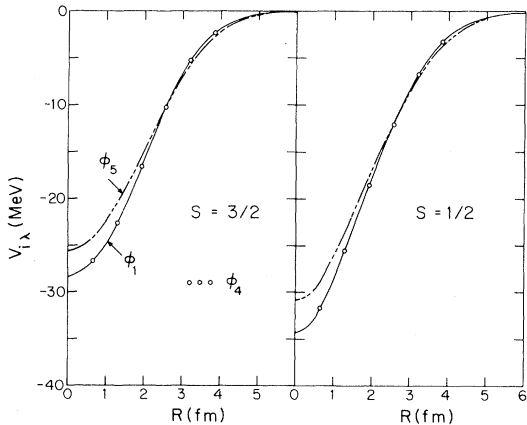


FIG. 3. Direct potentials $V_{i\lambda}$ in the quartet and doublet states.

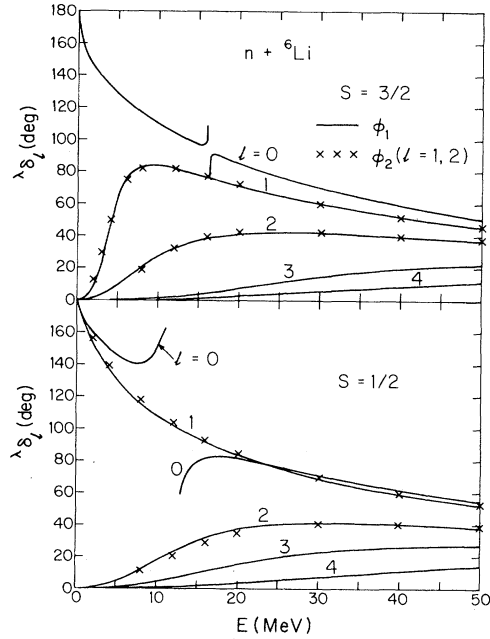


FIG. 4. Phase shifts ${}^\lambda\delta_l$ for $n + {}^6\text{Li}$ scattering, obtained with ${}^6\text{Li}$ internal functions ϕ_1 and ϕ_2 .

where the ${}^6\text{Li}$ wave function assumes a shell-model configuration in a single harmonic-oscillator well, the terms in these three groups reduce to type 1a, 1c, and 1d of our original classification of nucleon-exchange terms (for details, see Refs. 1 and 10).

As is well known, the direct potential $V_{i\lambda}$ is ob-

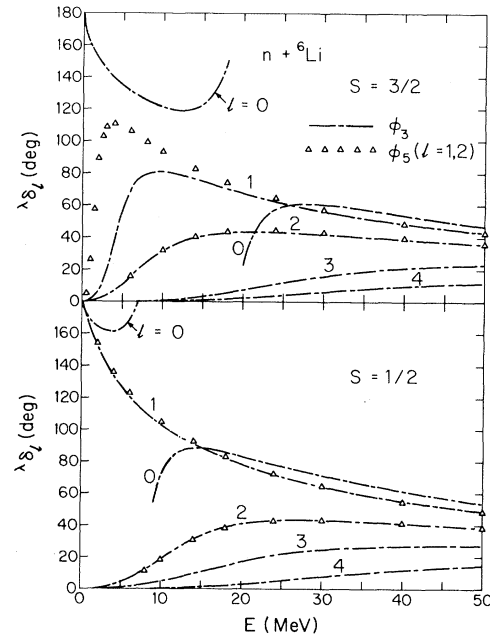


FIG. 5. Phase shifts ${}^\lambda\delta_l$ for $n + {}^6\text{Li}$ scattering, obtained with ${}^6\text{Li}$ internal functions ϕ_3 and ϕ_5 .

tained by a folding procedure involving the nucleon density distribution.³ Since all the type A functions yield very similar form-factor values for q^2 up to about 6 fm^{-2} , one anticipates that $V_{i\lambda}$ obtained with these functions should also be similar. This is shown in Fig. 3, where one finds that the direct potentials obtained with ϕ_1 and ϕ_4 are almost identical, but the direct potential obtained with the type B function ϕ_5 is appreciably different.

III. RESULTS

A. Bound states, phase shifts, and differential cross sections

Phase shifts ${}^\lambda\delta_l$ in the energy range 0–50 MeV are shown in Figs. 4 and 5. For clarity of presentation, only $l=1$ and 2 phases are plotted in the cases with ϕ_2 and ϕ_5 . Also, results obtained with ϕ_4 are not presented here, since these results have already been shown by the solid curves in Fig. 2 of Ref. 15.

The interesting features present in Figs. 4 and 5 are as follows:

(i) Phase shifts obtained with ϕ_1 and ϕ_2 are similar in all orbital angular-momentum and channel-spin states [except near spurious resonances; see (iii) below]. This is likely a consequence of the fact that these two type I functions yield similar $d + \alpha$ cluster correlations and form-factor values for ${}^6\text{Li}$.

(ii) Phase shifts obtained with the type I function ϕ_3 and the type II function ϕ_5 are quite different in the region of the ${}^4\text{P}$ resonance. This indicates that cluster correlations in ${}^6\text{Li}$ have a profound influence on the low-energy properties of the $n + {}^6\text{Li}$ system.

(iii) As expected, $l=0$ spurious or almost-forbidden states^{1,20} appear when the function ϕ_1 , ϕ_2 , ϕ_3 , or ϕ_4 is used in the calculation. In the case with ϕ_5 , such states do not exist, but there now occur redundant states at all energies. With ϕ_1 , ϕ_2 , ϕ_3 , and ϕ_4 , the spurious states are found to occur, respectively, at about 16, 17, 19, and 31 MeV for $s = \frac{3}{2}$, and at about 12, 16, 8, and 29 MeV for $s = \frac{1}{2}$. Here one notes that even the positions of these spurious resonance states seem to depend sensitively on the clustering properties of ${}^6\text{Li}$. It should be mentioned, however, that in light systems such resonances generally appear in an excitation-energy region where reaction channels make significant contributions. When these channels are taken into account, it has been found²¹ that the effects of these resonances do tend to become quite unimportant.

In Table I, we list the bound-state and resonance energies ${}^\lambda E_l$ of the ${}^2\text{P}$ and ${}^4\text{P}$ states, respectively. From this table, it is noted that the value of 4E_1 obtained with a type I function is around 4.4 MeV, which is appreciably different from that of around

TABLE I. Bound-state and resonance energies.

Type ${}^6\text{Li}$ function	I			II	
	ϕ_1	ϕ_2	ϕ_3	ϕ_4	ϕ_5
2E_1 (MeV)	-2.09	-2.45	-2.23	-2.44	-2.49
4E_1 (MeV)	4.40	4.26	4.67	1.89	1.78

1.8 MeV obtained with a type II function. This indicates that a proper consideration of the cluster correlations in ${}^6\text{Li}$ is indeed very important in determining the resonance energy of the ${}^4\text{P}$ state which is known to have predominantly an $n + {}^6\text{Li}$ cluster structure and, hence, can be reasonably described by our present calculation. For the ${}^2\text{P}$ bound state, the situation is rather different. The calculated values of 2E_1 turn out to be quite similar, independent of whether a type I or a type II ${}^6\text{Li}$ function is used. The reason for this is simple. The ${}^2\text{P}$ configuration in ${}^7\text{Li}$ represents the ground state having predominantly a ${}^3\text{H} + \alpha$ cluster structure which cannot, of course, be properly accounted for in a single-channel $n + {}^6\text{Li}$ study. Thus, a modification of the calculation by the introduction of $d + \alpha$ cluster correlations into the structure of ${}^6\text{Li}$ will have only a minor effect in this case and a more elaborate calculation is needed in order to adequately describe the ground state of ${}^7\text{Li}$.

Additional information may be obtained by studying the phase-shift behavior at a relatively high energy. In Table II, we list the results for $l=1$ to 4 at 40 MeV.²² Here, one finds that phase-shift values obtained with ϕ_1 , ϕ_2 , and ϕ_4 are similar, while those obtained with ϕ_3 and ϕ_5 are close to each other. The important point to note is that this similarity in the phase-shift feature occurs among wave functions classified according to type A or B, but not according to type I or II. This means that, when the energy is high, it is essential to choose a target wave function which adequately explains the form-factor characteristics. At such an energy, it seems that a

TABLE II. $n + {}^6\text{Li}$ phase shifts, in degrees, at 40 MeV.

Type ${}^6\text{Li}$ function	A			B	
	ϕ_1	ϕ_2	ϕ_4	ϕ_3	ϕ_5
${}^2\delta_1$	59.0	59.4	59.1	55.1	54.2
${}^2\delta_2$	40.2	40.2	40.1	41.1	41.0
${}^2\delta_3$	26.1	26.0	26.4	26.9	27.0
${}^2\delta_4$	11.0	10.6	11.3	11.8	12.0
${}^4\delta_1$	51.5	51.6	51.4	48.3	48.4
${}^4\delta_2$	39.7	40.3	40.3	38.8	39.2
${}^4\delta_3$	19.5	19.0	19.2	20.8	20.7
${}^4\delta_4$	8.6	8.4	8.9	9.6	9.5

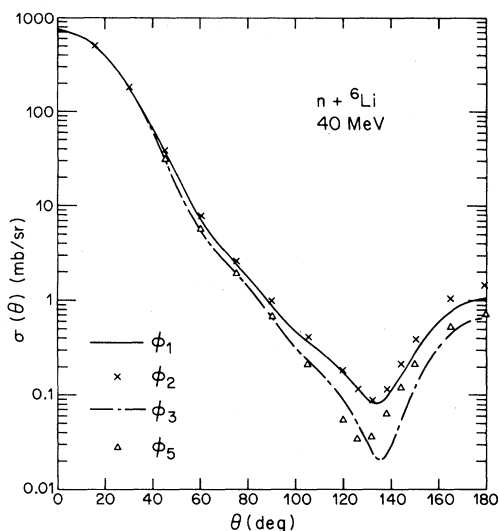


FIG. 6. Differential cross sections for $n + {}^6\text{Li}$ scattering at 40 MeV obtained with various ${}^6\text{Li}$ internal functions.

proper account of the target correlation behavior is of lesser importance.

The above finding may be further clarified by examining the scattering angular distribution at 40 MeV shown in Fig. 6. From this figure, one notes immediately that the results obtained with the type A functions ϕ_1 and ϕ_2 are nearly identical. The results obtained with the type B functions ϕ_3 and ϕ_5 are also rather similar, which is related to the fact that the form-factor values associated with these two functions are about the same up to q^2 of about 3 fm^{-2} . On the other hand, it can be clearly seen that the differential cross sections calculated with type A and type B functions are close to one another only at small angles, but begin to differ substantially at $\theta \geq 30^\circ$ where the momentum transfer becomes large. This confirms, therefore, that, at a high energy, the characteristics of the angular distribution can be reliably explained in the whole angular region only if the form-factor behavior of the target nucleus is correctly described over a wide q^2 range.

B. Discussion

In summary, we obtain, by examining the phase-shift and cross-section behavior, the following interesting findings:

(i) For a proper description of the resonance behavior of the $n + {}^6\text{Li}$ system in the low-energy region, the correlation property of ${}^6\text{Li}$ in terms of $d + \alpha$ clustering is of critical importance.

(ii) For a careful investigation of the $n + {}^6\text{Li}$ scattering behavior at high energies, one must adopt a ${}^6\text{Li}$ internal function which is flexible enough to

yield correct charge-form-factor values over a large range of q^2 .

To qualitatively explain finding (i), let us concentrate on the deuteron cluster. The neutron-proton correlation distance D of this cluster in ${}^6\text{Li}$, described by the internal function ϕ_1 , ϕ_2 , and ϕ_3 , is approximately given by

$$D \approx 2 \left(\frac{3}{4\bar{\alpha}} \right)^{1/2} = 2.4 \text{ fm} . \quad (19)$$

This means that, to effectively probe the presence of deuteron clustering, the incident neutron should have a reduced de Broglie wavelength λ close to 2.4 fm. Since the deuteron cluster is expected to appear predominantly in the surface region of ${}^7\text{Li}$, one may take the potential energy of the neutron as approximately equal to -5 MeV (see Fig. 3). Thus, for a neutron having a low energy of, say, 3 MeV, λ has a value around 1.8 fm, which is long enough to serve the purpose of probing the cluster structure of ${}^6\text{Li}$. On the other hand, when the energy is as high as 40 MeV, the value of λ becomes close to 0.7 fm, indicating that now the neutron will no longer be able to effectively detect the coherent structure of the two nucleons which constitute the deuteron cluster.

It is even simpler to understand finding (ii). The square of the momentum transfer to the neutron is

$$q^2 = 4k^2 \sin^2 \frac{1}{2} \theta , \quad (20)$$

where k is the neutron wave number and θ is the scattering angle. For $E = 40 \text{ MeV}$, q^2 is equal to 5.4 fm^{-2} when θ is taken to be 130° , the angle at which the cross-section minimum occurs²³ (see Fig. 6). This explains, therefore, that the ${}^6\text{Li}$ form-factor behavior up to q^2 of around 6 fm^{-2} must be properly accounted for when the 40-MeV $n + {}^6\text{Li}$ scattering data are considered. On the other hand, if one is contented in merely analyzing forward-angle data up to $\theta \approx 30^\circ$, then the q^2 values involved are less than 0.5 fm^{-2} and the requirement on the ${}^6\text{Li}$ wave function becomes much less severe.

IV. EXCHANGE EFFECTS

In a two-cluster A + B system, exchange effects have already been extensively studied^{10,11} when the internal function of each cluster is represented by a translationally-invariant shell-model configuration in a single harmonic-oscillator well. From these studies, we have obtained general conclusions concerning the contributions from class A and B nucleon-exchange terms (for details, see Ref. 11). In this investigation, our purpose is to see in what way these conclusions have to be modified when one adopts more complicated cluster internal functions

which take into account cluster correlations and which explain the characteristics of the form-factor behavior over a large q^2 region.

For the purpose mentioned above, we analyze the resonating-group results in terms of a simple potential model in which the ${}^6\text{Li}$ cluster is considered as a structureless particle interacting with the neutron through an E -, l -, and λ -dependent effective potential $\tilde{V}_{i\lambda}^i$ given by

$$\tilde{V}_{i\lambda}^i(R) = C_{i\lambda}^i V_{i\lambda}(R). \quad (21)$$

The parameter $C_{i\lambda}^i$ is then adjusted to yield the corresponding resonating-group phase-shift value in each (l, λ) state. Results at 40 MeV obtained with ϕ_2 (diamonds connected by solid lines), ϕ_4 (unconnected circles; $l=0$ values are not shown for the reason mentioned in Sec. III A), and ϕ_5 (triangles connected by dashed lines) are shown in Fig. 7. By examining the features contained in this figure, one may make the following assertions:

(i) The values of $C_{i\lambda}^i$ are quite similar for $i=2$ and 4, indicating again that, at such a relatively high energy, $d + \alpha$ cluster correlations in ${}^6\text{Li}$ seem to play a rather minor role.

(ii) The charge form factor of ${}^6\text{Li}$ does seem to have some influence. But, even here, one notes that the main characteristics of exchange contributions

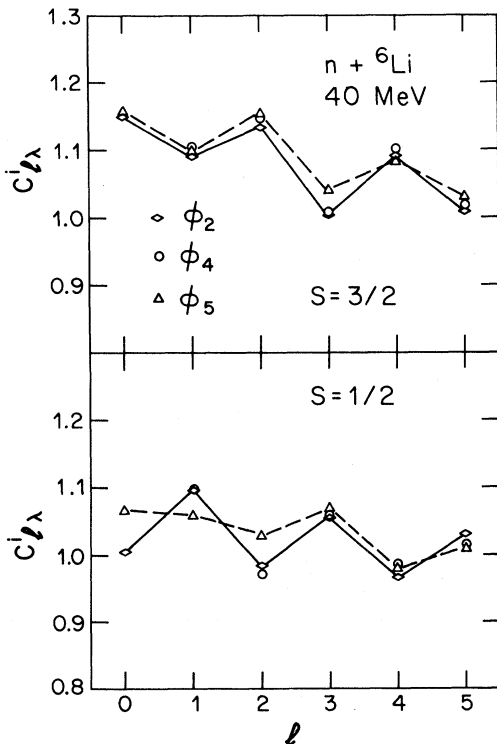


FIG. 7. $C_{i\lambda}^i$ as a function of l for $n + {}^6\text{Li}$ scattering at 40 MeV.

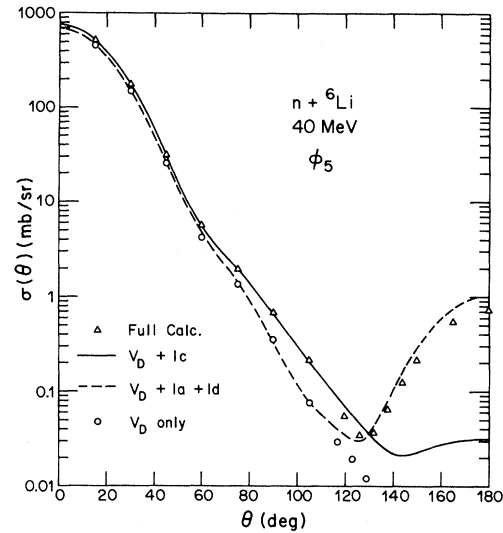


FIG. 8. Comparison of $n + {}^6\text{Li}$ differential cross sections at 40 MeV, obtained with the full resonating group, the $V_D + 1c$, the $V_D + 1a + 1d$, and the V_D -only calculations. The ${}^6\text{Li}$ internal function used is ϕ_5 .

remain unchanged; that is, the general magnitude and the odd-even l dependence of $C_{i\lambda}^i$ are rather similar in the cases obtained with the type A functions ϕ_2 and ϕ_4 on one hand and the type B function ϕ_5 on the other hand.

We must caution, however, that the above assertions may be specifically related to the comparatively simple nature of the $n + {}^6\text{Li}$ system. If one studies a more complicated system such as $\alpha + {}^6\text{Li}$ where the target nucleus contains a cluster having the same nucleon number and symmetry properties as the projectile nucleus, the resultant finding concerning the effects of target clustering could be somewhat different.

Next, we describe briefly the roles played by the various nucleon-exchange terms when the ${}^6\text{Li}$ functions ϕ_2 and ϕ_5 are used. For the type B (also type II) shell-model function ϕ_5 , it has been shown previously^{1,10} that these exchange terms may be classified according to the number x of nucleons interchanged between the neutron and the ${}^6\text{Li}$ cluster and the index q which denotes the interaction type. Thus, in the $n + {}^6\text{Li}$ system, we can discuss exchange effects in terms of type 1a, 1c, and 1d nucleon-exchange terms (for a detailed discussion of the type- xq term, see Ref. 1). In addition, it was discussed¹¹ that, at a relatively high energy greater than about 25 MeV/nucleon, the type 1c or knockon term²⁴ is a class A term which contributes mainly in the forward angular region, while the type 1a and 1d terms are class B terms which contribute mainly in the backward angular region. As is seen from Fig. 8,

this assertion is indeed fully borne out by our present calculation. In this figure, we show the differential-cross-section results at 40 MeV obtained with the full resonating-group calculation (open triangles), with V_D plus the type 1c term (solid curve), with V_D plus type 1a and 1d terms (dashed curve), and with the direct or no-exchange potential V_D alone (open circles). Here one finds that, in the angular region up to $\theta \approx 120^\circ$, the full resonating-group result can be well represented by a simpler calculation which involves only the direct and the type 1c terms. On the other hand, if one omits the type 1c term from the calculation, then the rise in cross section at backward angles can be reasonably accounted for, but the result at forward angles is not too satisfactory.

Similar analyses have also been carried out with the function ϕ_2 of type I and type A. In this case, the nucleon-exchange terms are classified into $\tilde{1}a$, $\tilde{1}c$, and $\tilde{1}d$ groups (see Sec. II B). The results are shown in Fig. 9. By comparing with Fig. 8, we note that there is a striking similarity. This indicates that, at least in the $n + {}^6\text{Li}$ system, the main properties of nucleon-exchange contributions do not seem to depend sensitively on the detailed nature of the cluster internal function.

V. CONCLUSION

The purpose of this investigation was to study the importance of utilizing, in a resonating-group calculation, flexible cluster internal functions which account for cluster correlations and which yield satisfactory values for the charge form factor. By examining the phase-shift and cross-section results in the $n + {}^6\text{Li}$ system, we obtain the interesting finding that, in the low-energy region, a proper consideration of the clustering properties of ${}^6\text{Li}$ is essential to explain the resonance behavior, while in the high-energy region one must choose a ${}^6\text{Li}$ internal function which reproduces the empirical form-factor result over a wide q^2 region.

Qualitative arguments are made to give a plausible explanation of the above finding. These arguments should be useful when one attempts to make a decision about the type of internal wave functions to be adopted in a more complicated problem. This will be important information to have, since the use of flexible cluster functions will generally increase to a large extent the amount of effort required in a resonating-group calculation.

Contributions from various nucleon-exchange terms have also been briefly studied. Here, it is found that the main characters of these contributions do not seem to be much affected by the clustering and form-factor properties of ${}^6\text{Li}$. This indi-

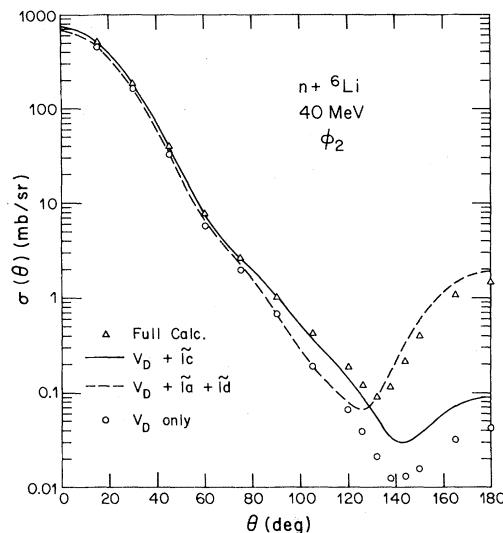


FIG. 9. Comparison of $n + {}^6\text{Li}$ differential cross sections at 40 MeV, obtained with the full resonating group, the $V_D + \tilde{1}c$, the $V_D + \tilde{1}a + \tilde{1}d$, and the V_D -only calculations. The ${}^6\text{Li}$ internal function used is ϕ_2 .

cates that the conclusions summarized in Ref. 11, based on studies in which the cluster internal function is represented by a shell-model configuration in a single harmonic-oscillator well, remain essentially unchanged and can be employed to discuss semi-quantitatively the importance of exchange effects in different situations.

The present investigation represents our initial effort to study the significance of taking target clustering into account in a scattering calculation. It has yielded useful results, but does have one unsatisfying aspect; that is, the neutron probe used here, being composed of a single nucleon, is only moderately effective in exploring the detailed properties of the ${}^6\text{Li}$ target. To reach more definitive conclusions, one should certainly perform further calculations in other systems, such as the $\alpha + {}^6\text{Li}$ or ${}^{16}\text{O} + {}^{18}\text{O}$ system in which heavier particles, namely, α and ${}^{16}\text{O}$ nuclei, are present as probing particles. Furthermore, we should also point out that there is another interesting reason to consider these particular systems. The target nuclei ${}^6\text{Li}$ and ${}^{18}\text{O}$ contain clusters which have the same nucleon numbers and symmetry properties as the incident nuclei. This may substantially affect the contribution from core-exchange terms, which have been shown, both theoretically¹¹ and experimentally,^{25,26} to be appreciable because the interacting nuclei have a small nucleon-number difference.

This research was supported in part by the U.S. Department of Energy under Contract No. DOE/DE-AC02-79 ER 10364.

- ¹Y. C. Tang, *Microscopic Description of the Nuclear Cluster Theory*, in *Lecture Notes in Physics* (Springer, Berlin, 1981), Vol 145.
- ²K. Wildermuth and Y. C. Tang, *A Unified Theory of the Nucleus* (Vieweg, Braunschweig, 1977).
- ³Y. C. Tang, M. LeMere, and D. R. Thompson, *Phys. Rep.* **47**, 167 (1978).
- ⁴K. Ikeda *et al.*, *Prog. Theor. Phys. Suppl.* **68**, 1 (1980).
- ⁵D. Baye, in *Proceedings of the International Conference on the Resonant Behavior of Heavy-Ion Systems, Aegean Sea—1980*, edited by G. Vourvopoulos (Nuclear Research Center “Democritos,” Athens, 1981).
- ⁶See, e.g., H. Kanada, T. Kaneko, and Y. C. Tang, *Nucl. Phys.* **A380**, 87 (1982).
- ⁷K. Langanke, *Phys. Lett.* **104B**, 112 (1981).
- ⁸L. R. Suelzle, M. R. Yearian, and H. Crannell, *Phys. Rev.* **162**, 992 (1967); G. C. Li, I. Sick, R. R. Whitney, and M. R. Yearian, *Nucl. Phys.* **A162**, 583 (1971); F. A. Bumiller, F. R. Buskirk, J. N. Dyer, and W. A. Monson, *Phys. Rev. C* **5**, 391 (1972).
- ⁹R. G. H. Robertson, P. Dyer, R. A. Warner, R. C. Melin, T. J. Bowles, A. B. McDonald, G. C. Ball, W. G. Davies, and E. D. Earle, *Phys. Rev. Lett.* **47**, 1867 (1981).
- ¹⁰M. LeMere and Y. C. Tang, *Phys. Rev. C* **19**, 391 (1979); M. LeMere, D. J. Stubeda, H. Horiuchi, and Y. C. Tang, *Nucl. Phys.* **A320**, 449 (1979); W. Sünkel and Y. C. Tang *ibid.* **A329**, 10 (1979); M. LeMere, Y. C. Tang, and H. Kanada, *Phys. Rev. C* **25**, 2902 (1982).
- ¹¹M. LeMere, Y. Fujiwara, Y. C. Tang, and Q. K. K. Liu, *Phys. Rev. C* **26**, 1847 (1982). Exchange effects have also been studied by other authors; see, e.g., D. Baye, J. Deenen, and Y. Salmon, *Nucl. Phys.* **A289**, 511 (1977); and K. Aoki and H. Horiuchi, *Prog. Theor. Phys.* **66**, 1508 (1981); **66**, 1903 (1981); **67**, 1236 (1982).
- ¹²There is no precise way to define the degree of nucleon clustering in a nucleus. By surface clustering we merely mean that, in a qualitative sense, the spatial overlap of the d and α clusters is not too strong.
- ¹³J. A. Koepke, R. E. Brown, Y. C. Tang, and D. R. Thompson, *Phys. Rev. C* **9**, 823 (1974).
- ¹⁴H. Kanada, T. Kaneko, and Y. C. Tang, *Nucl. Phys.* **A389**, 285 (1982).
- ¹⁵D. J. Stubeda, Y. Fujiwara, and Y. C. Tang, *Phys. Rev. C* **26**, 2410 (1982). The ${}^6\text{Li}$ rms charge radius calculated with ϕ_4 is 2.48 fm, which is slightly smaller than the value obtained with ϕ_1 , ϕ_2 , ϕ_3 , or ϕ_5 .
- ¹⁶The width parameter α for ϕ_α or ϕ_d in Eq. (17) is 0.514 fm⁻² for $i = 1, 2, 3$, but 0.278 fm⁻² for $i = 5$.
- ¹⁷The finding that β_3 is appreciably smaller than 1 [see Eq. (10)] is a rather clear indication that, in particular, the type I function ϕ_3 describes the ${}^6\text{Li}$ nucleus as having a considerable degree of $d + \alpha$ clustering. See the discussion in Y. C. Tang, K. Wildermuth, and L. D. Pearlstein, *Nucl. Phys.* **32**, 504 (1962); and V. G. Neudatchin and Yu. F. Smirnov, *Prog. Nucl. Phys.* **10**, 275 (1969).
- ¹⁸D. R. Thompson, M. LeMere, and Y. C. Tang, *Nucl. Phys.* **A286**, 53 (1977).
- ¹⁹The analytical derivation of the two-cluster and three-cluster kernels is rather complicated and will be described in detail in a later publication.
- ²⁰S. Saito, S. Okai, R. Tamagaki, and M. Yasuno, *Prog. Theor. Phys.* **50**, 1561 (1973).
- ²¹F. S. Chwieroth, Y. C. Tang, and D. R. Thompson, *Phys. Lett.* **46B**, 301 (1973).
- ²²Phase shifts for $l = 0$ are not listed, because the presence of spurious resonances greatly complicates the interpretation of the results.
- ²³It is not necessary to take θ larger than 130°, since the cross-section rise in the backward angular region comes mainly from core-exchange contributions.
- ²⁴G. R. Satchler and W. G. Love, *Phys. Rep.* **55**, 183 (1979).
- ²⁵D. Bachelier, M. Bernas, J. L. Boyard, H. L. Harney, J. C. Jourdain, P. Radvanyi, M. Roy-Stephan, and R. DeVries, *Nucl. Phys.* **A195**, 361 (1972).
- ²⁶W. von Oertzen and H. G. Bohlen, *Phys. Rep.* **19C**, 1 (1975).